The latent space of equational theories

Anonymous ACL submission

Abstract

Building on the collaborative Equational Theories project initiated by Terence Tao fifteen months ago, and combining it with ideas coming from machine learning and finite model theory, we construct a *latent space of equational theories* where each equational theory is located at a specific location, determined by its statistical behavior with respect to a large sample of finite magmas. This experiment enables us to observe for the first time how reasoning flows and produces surprisingly oriented and well-structured chains of logical implications in the latent space of equational theories.

> *Two things fill the mind with ever new and increasing admiration and awe, the more often and steadily we reflect upon them: the starry heavens above me and the moral law within me.*
>
> Immanuel Kant, Critique of Practical Reason.

1 Introduction

This work draws on the recent collaborative project Equational Theories (ET project) initiated by Terence Tao about fifteen months ago (Sept. 2024). In this innovative mathematical experiment, a large community of thirty-three authors exchanging on the Lean Zulip were able to describe *exhaustively* in only a few weeks the full implication preorder $(G, \Rightarrow)$ between 4694 basic equational theories on magmas, see (Bolan et al., 2024) for details.

Taking inspiration from the ET project and using the concept of *Stone pairing* originating from finite model theory (Nešetřil and Ossona de Mendez, 2020), we experiment with the idea that mathematical concepts (in this case, equational theories) can be located as *vertices in a latent space*, and then observed and mapped in the same way as constellations of stars in the sky.

Once the latent space of equational theories has been defined and constructed, we derive an *implication graph* $(G, \rightsquigarrow)$ from the full implication preorder $(G, \Rightarrow)$ made available online by the ET project. This allows us to observe that *reasoning flows in a surprisingly well-organized and oriented way* in the latent space of equational theories.

Despite its simple technical and conceptual design, this empirical study at the crossroad of mathematical logic and machine learning reveals the existence of a rich and well-organised *latent space of equational theories and reasoning flows* at the heart of universal algebra. We believe that the discovery of this emerging piece of mathematical landscape and the exploration of its remarkable geometric and statistical properties provide a nice illustration of the benefits of developing an experimental approach to logic.

Plan of the paper. After recalling in §2 the purpose of the ET project, we explain in §3 how we extract the graph $(G, \rightsquigarrow)$ of atomic steps from the implication preorder $(G, \Rightarrow)$. We then define in §4 the notion of Stone pairing from which we derive our feature space and then our latent space of equational theories in §5 and §6. A number of empirical observations on this latent space and on the flow of implications are made in §6, in §7 and §8. We describe related works and conclude in §9 and §10. We also describe the limitations of our work in §11.

2 The Equational Theories (ET) project

The purpose of the ET project (Bolan et al., 2024) was to describe entirely the implication order $(G, \Rightarrow)$ between the 4694 equational theories defined with *four instances at most* of the binary connective $\diamond$ on a given magma $(A, \diamond)$. This includes fundamental equational theories such as the *associativity law* (numbered as $\mathsf{Eqn}[4512]$ in the project) which involves three variables x, y, z and four instances of the connective:

$$\forall x, y, z \in A, \quad x \diamond (y \diamond z) \;=\; (x \diamond y) \diamond z$$

the *commutativity law* ($\mathsf{Eqn}[43]$) with two variables x, y and two instances of the connective:

$$\forall x, y \in A, \quad x \diamond y \;=\; y \diamond x$$

as well as the *idempotence law* (Eqn[3]) with one variable x and one instance of the connective:

$$\forall x \in A, \quad x = x \diamond x.$$

One methodological benefit of the exhaustive approach advocated by Tao is that other more exotic and largely unexplored equational theories suddenly appear as meaningful. An example is provided by the *Obelix law* (Eqn[1491]) with four instances of the connective:

$$\forall x, y \in A, \quad x = (y \diamond x) \diamond (y \diamond (y \diamond x))$$

and the *Asterix law* (Eqn[65]) with three instances of the connective:

$$\forall x, y \in A, \quad x = (y \diamond (x \diamond (y \diamond x)))$$

Indeed, the Asterix law implies the Obelix law for all *finite magmas* although it is possible to find an *infinite magma* $(A, \diamond)$ which satisfies the Asterix law without satisfying the Obelix law:

$$(A, \diamond) \models \mathsf{Eqn}[65] \quad \text{and} \quad (A, \diamond) \not\models \mathsf{Eqn}[1491].$$

where the symbol $\models$ expresses the fact that the magma $(A, \diamond)$ satisfies a given equational law. This establishes that there is no proof that Eqn[65] implies Eqn[1491], see (Bolan et al., 2024) for details.

3 First step: building the graph $(G, \rightsquigarrow)$

3.1 The implication preorder $(G, \Rightarrow)$

We start from the the implication preorder produced by the ET project, which has **4694** elements, one for each equational theory considered in the project. This means that the number of possible implications between equations is

$$4\,694 \times 4\,694 = 22\,033\,636$$

It was established by the members of the ET project that the actual number of implications is

$$\mathbf{8\,178\,279} \approx 0.37 \times 22\,033\,636$$

An implication between equational theories

$$\mathsf{Eqn}[j] \Rightarrow \mathsf{Eqn}[k]$$

is called *reversible* when the converse implication

$$\mathsf{Eqn}[k] \Rightarrow \mathsf{Eqn}[j]$$

holds. We say in that case that the two equational theories are *provably equivalent* and write

$$\mathsf{Eqn}[j] \sim \mathsf{Eqn}[k].$$

This defines an equivalence relation $\sim$ which partitions the set of $4\,694$ vertices into equivalence classes which we call *reversible cliques*. Among the implications of the preorder $(G, \Rightarrow)$, there are

$$\mathbf{5\,702\,669} \approx 0.70 \times 8\,178\,279$$

strict implications and

$$\mathbf{2\,475\,610} \approx 0.30 \times 8\,178\,279$$

reversible implications (including the $4\,694$ self-references).

3.2 The implication graph $(G, \rightsquigarrow)$

Starting from the implication preorder $(G, \Rightarrow)$ provided by the ET project, we construct a directed graph $(G, \rightsquigarrow)$ of *atomic steps*. A strict implication

$$\mathsf{Eqn}[j] \Rightarrow \mathsf{Eqn}[k]$$

is called *atomic* when it cannot be decomposed, in the sense that, for all equational theories $\mathsf{Eqn}[\ell]$,

$$\mathsf{Eqn}[j] \Rightarrow \mathsf{Eqn}[\ell] \quad \text{and} \quad \mathsf{Eqn}[\ell] \Rightarrow \mathsf{Eqn}[k]$$

implies that

$$\mathsf{Eqn}[j] \sim \mathsf{Eqn}[\ell] \quad \text{or} \quad \mathsf{Eqn}[\ell] \sim \mathsf{Eqn}[k].$$

We write in that case:

$$\mathsf{Eqn}[j] \rightsquigarrow \mathsf{Eqn}[k]$$

Note that a strict implication

$$\mathsf{Eqn}[j] \Rightarrow \mathsf{Eqn}[k]$$

holds if and only if there exists a path

$$\mathsf{Eqn}[j] \rightsquigarrow \cdots \rightsquigarrow \mathsf{Eqn}[k]$$

of atomic steps. It is also worth observing that the notion of atomic step is not intrinsic, and depends on the set of equational theories considered in the ET project. The number of atomic steps, or arrows, in the graph $(G, \rightsquigarrow)$ is

$$\mathbf{1\,052\,209} \approx 0.18 \times 5\,702\,669$$

3.3 The implication graph $(G, \rightsquigarrow)$ modulo

One remarkable property of atomic steps is that they are closed under reversible implications, in the sense that every atomic step $\mathsf{Eqn}[j] \rightsquigarrow \mathsf{Eqn}[k]$ and provably equivalent equational theories with the source and target

$$\mathsf{Eqn}[j'] \sim \mathsf{Eqn}[j] \qquad \mathsf{Eqn}[k] \sim \mathsf{Eqn}[k']$$

induces another atomic step $\mathsf{Eqn}[j'] \rightsquigarrow \mathsf{Eqn}[k']$. For that reason, we declare that two atomic steps

$$\mathsf{Eqn}[j] \rightsquigarrow \mathsf{Eqn}[k] \qquad \mathsf{Eqn}[j'] \rightsquigarrow \mathsf{Eqn}[k']$$

are equivalent modulo $\sim$ when $\mathsf{Eqn}[j] \sim \mathsf{Eqn}[j']$ and $\mathsf{Eqn}[k] \sim \mathsf{Eqn}[k']$. We obtain in this way a directed acyclic graph noted $(G, \rightsquigarrow)/\sim$

with **1415** vertices and **4824** arrows

defined as equivalence classes of vertices and arrows of $(G, \rightsquigarrow)$ modulo $\sim$.

4 Stone pairing

We find useful to recall the notion of *Stone pairing* introduced by (Nešetřil and Ossona de Mendez, 2012, 2020) in the field of finite model theory, see also (Gehrke et al., 2022) for a discussion. We will see in §5 and §6 that our definition of the feature space and of the latent space of equational theories

relies on this *probabilistic* variant of validity of a first-order formula φ in a model A. Here, we focus on the *first-order theory of magmas* defined by the signature $\{\diamond : 2\}$ for the binary function $\diamond$. Recall that a magma $(A, \diamond)$ is defined as a set A equipped with a binary operation

$$\diamond \ : \ A \times A \longrightarrow A.$$

A typical first-order predicate φ states the existence of a neutral element:

$$\exists e. \forall x. \quad \big(x \diamond e = x \ \wedge \ e \diamond x = x \big)$$

or the existence of a right residual for any pair of elements x, z of the magma:

$$\forall x. \forall z. \exists y. \quad x \diamond y = z.$$

All equations between magmas can be expressed in that way. Typically, $\mathsf{Eqn}[3721]$ of the equational theory project can be written as the formula

$$\varphi(x, y) \quad \equiv \quad x \diamond y \ = \ (x \diamond y) \diamond (x \diamond y).$$

with two free variables x, y. Now, given a finite magma $(A, \diamond)$ and a first-order formula

$$\varphi(x_1, \ldots, x_n)$$

with n free variables $x_1, \ldots, x_n$, the Stone pairing

$$\langle \, \varphi \, | \, A \, \rangle \ \in \ [0, 1]$$

is the scalar defined as the probability:

$$\frac{\#\left\{ (a_1, \ldots, a_n) \in A^n \mid \varphi(a_1, \ldots, a_n) \, \text{holds} \right\}}{\#A^n}$$

that a n-tuple of elements

$$(a_1, \ldots, a_n) \in A^n$$

satisfies the n-ary formula φ. Here we write $\#A$ for the cardinal of a finite set A. By way of illustration, observe that

$$A \ \vDash \ \forall \mathbf{x}, \varphi(\mathbf{x}) \quad \Longleftrightarrow \quad \langle \, \varphi(\mathbf{x}) \mid A \, \rangle \ = \ 1$$

where we write $A \vDash \psi$ when a first-order formula ψ is satisfied by a given magma A, and use the notation $\mathbf{x} = x_1, \ldots, x_n$ for the sequence of free variables of the formula φ. From this follows in particular that

$$\langle \, x = x \mid A \, \rangle \ = \ 1$$

for every finite magma A. Fractional values different from 0 and 1 are the most common in practice. For instance, note that

$$\langle \, x = y \mid A \, \rangle \ = \ \frac{1}{\#A}$$

for every finite magma A, since there is a probability of one divided by the cardinal of A that two elements $a_1, a_2 \in A$ happen to be equal.

5 The feature space of equational theories

In this section, we explain how we use the probabilistic concept of Stone pairing in order to construct our latent space of equational theories.

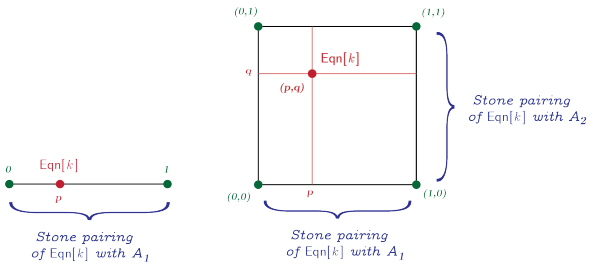

Figure 1: How each equation $\mathsf{Eqn}[k]$ is assigned a position in the hypercube $\mathbb{H}_n$ of dimension $n = \#\mathsf{Mags}$ the number of sampled finite magmas $A_1, \ldots, A_n$.

5.1 The generation process

We proceed in the following way. We start by generating a large number $n = \#\mathsf{Mags}$ of finite magmas $A_1, \ldots, A_n$ of a fixed size N. For simplicity, we define them with the same underlying set $\{0, \ldots, N-1\}$. Each magma A_ℓ for $1 \leq \ell \leq n$ is thus generated as a two-dimensional array of size $N \times N$, where each entry is a randomly chosen value between 0 and $N-1$. This two-dimensional array describes the multiplication table of the magma $A_\ell = \{0, \ldots, N-1\}$ and thus completely characterizes it. We typically work with a sample of $n = 1000$ magmas of size N between 4 and 16. These numbers $n = 1000$ and $4 \leq N \leq 16$ appear reasonable from a computational point of view and sufficient for our purposes.

5.2 The feature hypercube $\mathbb{H}_n = [0, 1]^n$

We define a matrix of size $\#\mathsf{Eqns} \times \#\mathsf{Mags}$

$$R \quad = \quad \big(p_{k,\ell} \big)_{k \in \mathsf{Eqns}, \ell \in \mathsf{Mags}} \qquad (1)$$

where $\#\mathsf{Eqns} = 4964$ is the number of equations and $n = \#\mathsf{Mags} = 1000$ is the number of sampled magmas of size N. Each entry $p_{k,\ell}$ of the matrix R is defined as the probability

$$p_{k,\ell} \quad = \quad \langle \, \mathsf{Eqn}[k] \, | \, A_\ell \, \rangle$$

given by the Stone pairing of $\mathsf{Eqn}[k]$ with the finite magma A_ℓ. Every equation $\mathsf{Eqn}[k]$ induces a line or vector of n probabilities

$$\big(p_{k,1} \ , \ \cdots \ , \ p_{k,n} \big) \ \in \ [0, 1]^n$$

which defines an element of the hypercube $\mathbb{H}_n = [0, 1]^n$ of dimension $n = \#\mathsf{Mags}$, see Fig. 1 for an illustration.

5.3 Stone spectrum

The hypercube $\mathbb{H}_n = [0, 1]^n$ comes equipped with an action

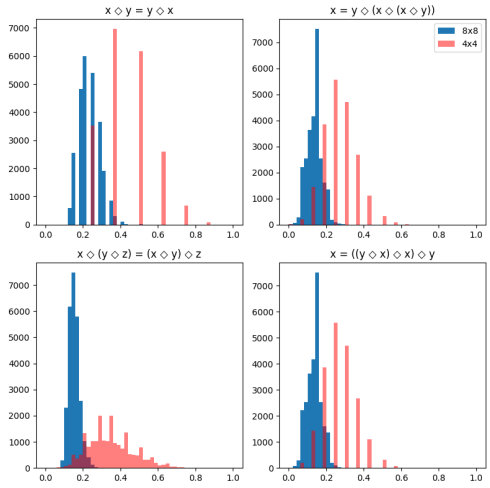

Figure 2: Stone spectra of the commutative law (top-left) and of the associative law (bottom-left) for a sampling of $n = 20\,000$ magmas of size 4 (red curve) and of $n = 24\,000$ magmas of size 8 (blue curve). The Stone spectra of the conjugate theories Eqn[63] and Eqn[271] are identical (top and bottom, right).

$$\circledast \quad : \quad S_n \times \mathbb{H}_n \longrightarrow \mathbb{H}_n$$

of the symmetry group S_n on the n dimensions (or directions) of the space $\mathbb{H}_n$, defined as

$$\sigma \circledast (p_1, \ldots, p_n) := (p_{\sigma(1)}, \ldots, p_{\sigma(n)})$$

for $\sigma \in S_n$ and $\mathbf{p} = (p_1, \ldots, p_n) \in \mathbb{H}_n$. Since the sampling order of the magmas $A_1, \ldots, A_n$ does not matter, it makes sense to consider the position of each equational theory

$$\mathbf{p} := (p_1, \ldots, p_n) \in \mathbb{H}_n$$

modulo the action of the symmetry group S_n. One obtains in this way a position in the quotient space $\mathbb{H}_n/S_n$, defined as the multiset

$$\mathbf{p}\,[S_n] \;:=\; \{\!|\, p_1 \,,\, \ldots \,,\, p_n \,|\!\}$$

We call this multiset the *Stone spectrum* of the equational theory. The Stone spectrum can be nicely visualized as a finite positive measure of weight n on the interval $[0, 1]$, defined as the sum

$$\sum_{i=1}^{n} \delta_{p_i}$$

of the Dirac distributions δ_{p_i}, see Fig. 2 for an illustration.

5.4 Stone interference spectrum

The cartesian product of the hypercube $\mathbb{H}_n = [0, 1]^n$ with itself comes equipped with an action

$$\circledast \quad : \quad S_n \times \mathbb{H}_n \times \mathbb{H}_n \longrightarrow \mathbb{H}_\times \mathbb{H}_n$$

defined componentwise:

$$\sigma \circledast (\mathbf{p}, \mathbf{q}) \;:=\; (\sigma \circledast \mathbf{p}, \sigma \circledast \mathbf{q})$$

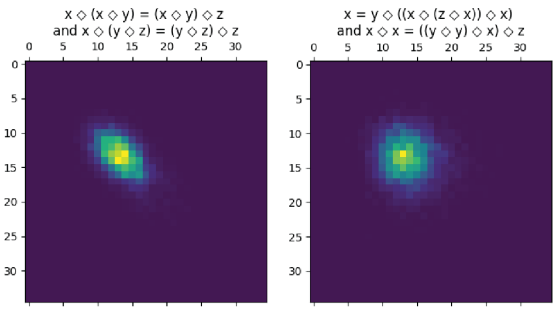

Figure 3: The Stone interference spectrum of Eqn[4400] and Eqn[4533] detects a degree of statistical dependence between the two conjugate equational theories (left) while the Stone interference spectrum of Eqn[1092] and Eqn[4092] shows full statistical independence between the two equational theories (right).

Instead of looking at the relative positions of a pair of equational theories Eqn[j] and Eqn[k] in the feature space $\mathbb{H}_n \times \mathbb{H}_n$, we may look at their relative positions in the quotient space $\mathbb{H}_n \times \mathbb{H}_n/S_n$. This is provided by the finite multiset of pairs:

$$(\mathbf{p}, \mathbf{q})\,[S_n] \;:=\; \{\!|\, (p_1, q_1) \,,\, \ldots \,,\, (p_n, q_n) \,|\!\}$$

which we call *Stone interference spectrum*. In the same way as the Stone spectrum of an equational theory, this interference spectrum of two equational theories can be described as the finite measure on the square $[0, 1]^2$ defined as the sum

$$\sum_{i=1}^{n} \sum_{j=1}^{n} \delta_{(p_i, q_j)}$$

where $\delta_{(p,q)}$ denotes the Dirac distribution of $(p, q) \in [0, 1]^2$. This representation enables one to visualize the Stone interference spectrum in an instructive way, see Fig. 2 for two illustrations.

6 The latent space of equational theories

6.1 Building the latent space using a PCA dimensionality reduction

We apply a principal component analysis (PCA) method in order to derive a 3-dimensional representation of the 4694 equational theories from thr positions in the n-dimensional feature space $\mathbb{H}_n$. We thus start by computing the center of gravity $\mu \in \mathbb{H}_n$ of the 4694 vertices in $\mathbb{H}_n$. We subtract μ from each column of the matrix R defined in (1), in order to obtain a matrix $X = R - \mu$ with zero-mean rows. The PCA method then diagonalizes the covariance matrix $C_X = \frac{1}{n} X X^T$, see (Shlens, 2014; Hanchi et al., 2025) for details.

We keep the first three principal components or dimensions (noted X, Y, Z) of the row-space which we call the *latent space of equational theories*. This

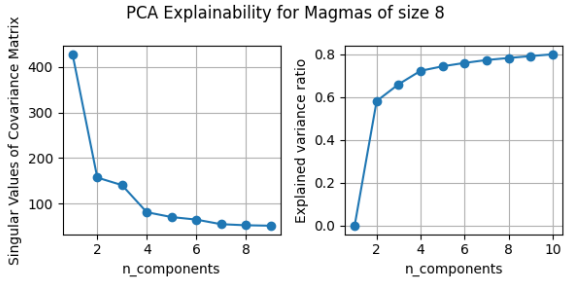

Figure 4: PCA Explainability statistics for a random sample of $n = 20\,000$ magmas of size 8. The values of the first ten singular values (left) and the explained variance ratio (right) for the first ten principal components.

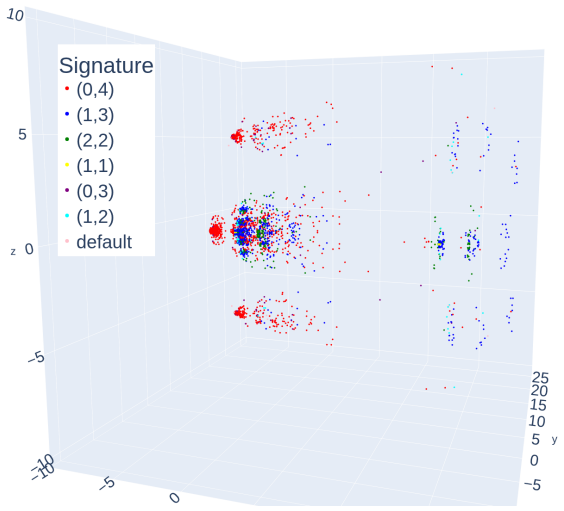

Figure 5: Latent space of equational theories where every theory is colored according to its signature (a, b), where a and b are the numbers of diamond operations on the lefthand and righthand side of the theory.

choice of picking the three first dimensions of the PCA is justified by our visualization purposes as well as by the fact that a majority of variability in the data is captured by the first three principal components, as shown in Fig. 4.

6.2 The latent space is good at detecting signatures of equational theories

Exploring the latent space and looking at each position of the 4964 equational theories, we observe that the latent space is surprisingly good at identifying and grouping together the equational theories $\mathsf{Eqn}[k]$ with the same signature, see Fig. 5.

Here, by signature of an equational theory, we mean the ordered pair (a, b) describing the numbers a and b of diamonds on the left-hand side and right-hand side of the equation, respectively. Typically, the Tarski's law $\mathsf{Eqn}[542]$

$$x = (z \diamond (x \diamond (y \diamond z)))$$

has signature $(0, 3)$. We indicate how the 4694 equational theories are partitioned according to their signature, and how they are colored in the latent space depicted in Fig. 5.

2842	theories have signature	$(0, 4)$	[red]
1015	theories have signature	$(1, 3)$	[blue]
427	theories have signature	$(2, 2)$	[green]
260	theories have signature	$(0, 3)$	[purple]
104	theories have signature	$(1, 2)$	[cyan]
30	theories have signature	$(0, 2)$	[pink]
9	theories have signature	$(1, 1)$	[yellow]
5	theories have signature	$(0, 1)$	[pink]
2	theories have signature	$(0, 0)$	[pink]

6.3 Expectation and variance

The *expectation* and *variance* of an equational theory $\mathsf{Eqn}[k]$ are defined as the expectation and variance of the associated sequence of Stone pairings:

$$E[\,\mathsf{Eqn}[k]\,] = \tfrac{1}{n}\textstyle\sum_{i=1}^{n} p_i$$
$$V[\,\mathsf{Eqn}[k]\,] = \tfrac{1}{n}\textstyle\sum_{i=1}^{n} \Big(p_i - E[\,\mathsf{Eqn}[k]\,]\Big)^2$$

where $p_i = \langle\, \mathsf{Eqn}[k] \,|\, A_i \,\rangle$. Note that the expectation and variance do not depend on the sampling order of the finite magmas $A_1, \ldots, A_n$ and can be thus computed from the Stone spectrum of $\mathsf{Eqn}[k]$.

6.4 The X-axis is strongly correlated to expectation

The first principal component X of a theory $\mathsf{Eqn}[k]$ is strongly correlated to its expectation $E[\,\mathsf{Eqn}[k]\,]$, as shown by the linear regression graph, see Fig. 8 in Appendix. As a consequence, the theory with maximum X-value is $\mathsf{Eqn}[0]$

$$x = x$$

with expectation exactly 1, followed by $\mathsf{Eqn}[3277]$ and its conjugate $\mathsf{Eqn}[4067]$

$$x \diamond x = ((x \diamond x) \diamond y) \diamond y$$
$$x \diamond x = y \diamond (y \diamond (x \diamond x))$$

whose expectation in the sample of finite magmas of size 8 we took is around .46. On the other side of the latent space, one of the equational theories with smallest X-value is $\mathsf{Eqn}[1]$

$$x = y$$

with expectation exactly $\frac{1}{8} = .125$ in any finite magma of size $N = 8$ used in the sample.

6.5 The Y-axis is correlated to variance

The principal component Y of an equational theory $\mathsf{Eqn}[k]$ is strongly correlated to its variance $V[\,\mathsf{Eqn}[k]\,]$, as shown by the linear regression, see Fig. 9 in Appendix. The equational theory with minimum variance and Y-value is $\mathsf{Eqn}[4275]$ and conjugate $\mathsf{Eqn}[4590]$:

$$x \diamond (x \diamond x) \;=\; y \diamond (y \diamond y)$$
$$(x \diamond x) \diamond x \;=\; (y \diamond y) \diamond y$$

The equational theory with maximum variance and Y-value is $\mathsf{Eqn}[3658]$ which is self-conjugate:

$$x \diamond x \;=\; (x \diamond x) \diamond (x \diamond x)$$

6.6 The Z-axis detects conjugacy

One immediate and striking observation on the latent space is the Z-value produces a reflection symmetry between conjugate theories, around the plane $Z = 0$. We noticed this emerging reflection symmetry between conjugate theories in our first experiments, and improved this reflection symmetry by selecting a perfectly symmetric sample of finite magmas. For reference, the equational theory with maximum Z-value is $\mathsf{Eqn}[1022]$

$$x \;=\; x \diamond ((x \diamond (x \diamond y)) \diamond y)$$

closely followed by $\mathsf{Eqn}[428]$

$$x \;=\; x \diamond (y \diamond (x \diamond (y \diamond x)))$$

By reflection symmetry, the theory with minimum Z-value is the conjugate $\mathsf{Eqn}[2529]$:

$$x \;=\; (y \diamond ((y \diamond x) \diamond x) \diamond x$$

closely followed by the conjugate $\mathsf{Eqn}[3067]$:

$$x \;=\; (((x \diamond y) \diamond x) \diamond y) \diamond x$$

Accordingly, there are 84 self-conjugate equational theories and they all appear on the plane $Z = 0$. This ability of the Z-component to detect conjugacy is remarkable since two conjugate theories $\mathsf{Eqn}[j]$ and $\mathsf{Eqn}[k]$ have the same Stone spectrum, and thus the same expectation and variance, see the definition in §5.3 and discussion in §6.3.

7 Clustering of provably equivalent theories in the latent space

Now that we have constructed the latent space of equational theories, we can embed the implication graph $(G, \rightsquigarrow)$ to visualize what it looks like in three dimensions. For every pair of equational theories related by a proof $\mathsf{Eqn}[j] \Longrightarrow \mathsf{Eqn}[k]$ we thus draw an *edge* $\mathsf{Eqn}[j] \longrightarrow \mathsf{Eqn}[k]$ between the vertices associated to $\mathsf{Eqn}[j]$ and $\mathsf{Eqn}[k]$ in the latent space. We use the same terminology as for implications, and thus distinguish three classes of edges: the *reversible* edges $\sim$, the *atomic* edges $\rightsquigarrow$ which are strict by definition, and the *strict* edges $\Rightarrow$ which are general and not necessarily atomic. The length of an edge can be computed in several ways. In this paper, we choose the simplest distance which is the Euclidian distance in the latent space.

At this stage, it is important to notice that two provably equivalent theories $\mathsf{Eqn}[j]$ and $\mathsf{Eqn}[k]$ may induce different Stone pairings within a given finite magma $(A, \diamond)$. Indeed, $\mathsf{Eqn}[j] \sim \mathsf{Eqn}[k]$ simply ensures that validity is preserved

$$(A, \diamond) \vDash \mathsf{Eqn}[j] \iff (A, \diamond) \vDash \mathsf{Eqn}[k]$$

in other words, that the Stone pairing of $\mathsf{Eqn}[j]$ is equal to 1 if and only if the Stone pairing of $\mathsf{Eqn}[k]$ is equal to 1. On the other hand, we observe empirically that the reversible edges are on average seven times shorter than strict atomic edges, and ten times shorter than general stric edges, as indicated in the table below.

	Reversible	**Atomic**	**Strict**
count	2 470 916	1 052 209	5 707 363
mean	0.69	5.29	7.17
std	0.65	2.22	4.30
min	0.00	0.00	0.00
25%	0.00	4.14	4.17
50%	0.63	4.69	6.14
75%	0.96	6.33	9.22
max	5.36	37.08	41.20

This important difference suggests a degree of clustering of the provably equivalent theories in the latent space. The hypothesis can be validated by computing the center of mass of each clique of provably equivalent theories, and connecting each theory to the center of mass of its corresponding clique. One obtains in this way a three-dimensional picture, see Fig. 6, where the clusters of provably equivalent theories are clearly separated.

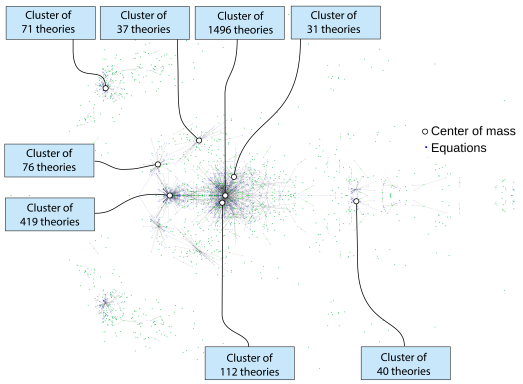

Figure 6: Visualizing the center of mass of each provably equivalent clique. Each equational theory is drawn connected to its corresponding center of mass.

8 Implication flows in the latent space

The clustering of provably equivalent theories in the latent space observed in §7 has an important

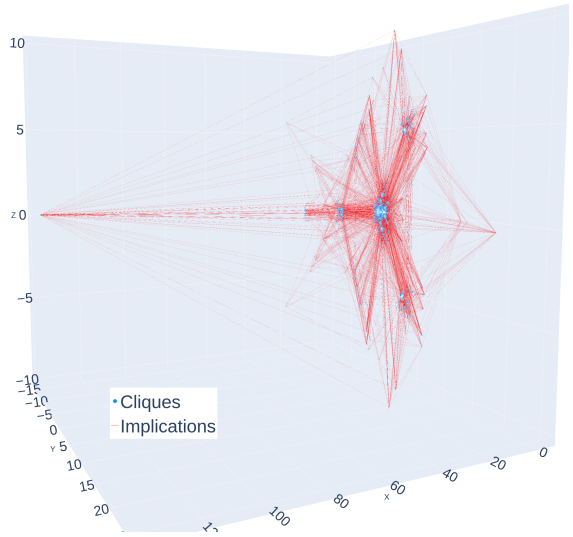

Figure 7: A global view of the latent space of equational theories and of the 1415 vertices and 4824 edges of the implication graph $(G, \rightsquigarrow)$ modulo reversibility. The existence of implication flows reveals an emerging similitude between the model-theoretic definition of the latent space and the proof-theoretic definition of the implication graph.

consequence: it enables us to derive from the original embedding of $(G, \rightsquigarrow)$ an embedding of the graph $(G, \rightsquigarrow)$ modulo $\sim$. The idea is to replace each reversible clique modulo $\sim$ by a single ball located at the center of mass of the associated cluster. The number of provably equivalent theories in the clique is indicated by the diameter of the ball. One obtains in that way a graph with 1415 vertices (blue balls of different diameters) and 4824 edges (red arrows), see Fig. 7.

We mention a number of remarkable emerging phenomena which appear when one observes the embedding of the graph $(G, \rightsquigarrow)$ modulo $\sim$.

8.1 Radial direction of implication flows

A striking observation on the picture of Fig. 7 is the existence of clearly oriented implication flows across the latent space. The mainstream direction goes along the X-axis towards equational theories with higher expectations. There is also a clear radial orientation along the Y and Z-axis towards theories with higher variance, and with different degrees of self-conjugacy.

The implication graph looks disorganised close to the source $\mathsf{Eqn}[1]$ which implies all the other theories. On the other hand, it looks very organised close to the sink $\mathsf{Eqn}[0]$ which is implied by every theory. One tentative explanation is that more equational theories $\mathsf{Eqn}[k]$ such as *idempotency* or *commutativity* can be deduced as consequences of a theory $\mathsf{Eqn}[j]$ closer to the source. These equational theories can be used in the reasoning to establish unexpected facts, and produce disorganised edges. On the other hand, when one gets closer to the sink, it becomes much more difficult to prove things, and this could explain why there are so few implication edges going against the mainstream radial orientation

8.2 Parallelism of implications

Another striking phenomenon is that many implication edges appear to be similar and parallel in the latent space. A closer inspection shows that very often, the parallel edges have similar source and target theories. An illustration is provided by the pair of parallel implications

$$\begin{array}{c} \mathsf{Eqn}[422] \Longrightarrow \mathsf{Eqn}[2851] \\ \mathsf{Eqn}[427] \Longrightarrow \mathsf{Eqn}[2861] \end{array}$$

where $\mathsf{Eqn}[422]$ and $\mathsf{Eqn}[427]$ are very similar:

$$\begin{array}{l} \forall x.y.z. \quad x = x \diamond (x \diamond (y \diamond (z \diamond y))) \\ \forall x.y.z. \quad x = x \diamond (y \diamond (x \diamond (x \diamond z))) \end{array}$$

and for $\mathsf{Eqn}[2851]$ and $\mathsf{Eqn}[2861]$:

$$\begin{array}{l} \forall x.y. \quad x = ((x \diamond (x \diamond y)) \diamond x) \diamond x \\ \forall x.y. \quad x = ((x \diamond (y \diamond x)) \diamond x) \diamond x \end{array}$$

We conjecture that this parallelism phenomenon is related to the Herbrand theorem in formal logic, see (Miller, 1987) and the discussion in Appendix. Note in particular that the witnesses (or expansion trees) provided by the Herbrand theory generalise the notion of *simple rewrite* elaborated and collected in Section 21 of the ET project blueprint. In that prospect, it would be worth collecting a large number of such parallel edges in the latent space and exploring how the underlying proofs are related, typically by inspecting their expansion trees, to see whether our conjecture holds. We leave that for future work.

8.3 Contrarian edges and hard implications

After observing the mainstream orientation of implication flows, we looked for atomic edges with a minority or contrarian orientation. To that purpose, we searched and collected a number of *longest paths* in the implication graph $(G, \rightsquigarrow)$ modulo $\sim$. Among these paths, we observed some unexpected behaviours like *swirls around the cliques or clusters* of provably equivalent theories. A possible explanation is that these clusters of provably equivalent theories are *active proof-theoretic areas* of the latent space, where many different equivalent

formulations of the very same concept can be established by back-and-forth: of the form:

$$\mathsf{Eqn}[j] \Longrightarrow \mathsf{Eqn}[k] \Longrightarrow \mathsf{Eqn}[j]$$

as we observed empirically.

We also considered the hard implications mentioned on Section 27 of the ET project blueprint as well as the implications with long Vampire times. We noticed empirically that a number of them had unusual and contrarian shapes as atomic edges in the latent space. At the same time, we are not entirely sure of the phenomenon at this stage, and we could not develop a sufficiently clear and complete picture of it. We thus prefer to leave this important and promising line of investigation for future work.

9 Related works

An important question underlying our work is whether (and how) the latent information provided by finite model theory is related to the proof-theoretic structure witnessed by the implication graph. From that point of view, it would be instructive to experiment with the convolutional neural network (CNN) model developed in the ET project (Bolan et al., 2024) and see whether it can be improved by integrating the latent space structure coming from Stone pairings.

Our exploration of the connection between proof theory and finite model theory is driven by the desire to understand the latent, statistical and distributional structure of deduction in machine learning, and we hope that it will bring new insights on the way large language models reason internally in their own latent space (Asperti et al., 2025; Zhou et al., 2025). From that point of view, it is very much in line and inspired by the dualistic approach to type theory and language developed in (Gastaldi and Pellissier, 2021, 2023), see also the more recent (Bradley et al., 2024).

10 Conclusion and future work

This work started as a small-scale exercise in experimental logic, building on the achievements of the Equational Theories project initiated by Terence Tao fifteen months ago, and on the exhaustive description of the implication preorder $(G, \Rightarrow)$ between 4694 equational theories established by this remarkably active and lively collaborative project.

Our plan was to proceed in two stages. In a first stage, we would define a latent space of the 4694 equational theories using ideas and methods coming from machine learning and finite model theory. Then, in a second stage, we would study the geometric (and metric) properties of the implication preorder $(G, \Rightarrow)$ of equational theories seen as *embedded* in the latent space just constructed.

The project was propelled since its origins by curiosity and exploratory joy, combined with the hope and desire of revealing meaningful hidden latent structures at the heart of mathematical reasoning. Despite the preliminary nature and technical simplicity of this work, the outcome of the experiment largely exceeds what we originally expected:

1. First, we observed with great surprise that the latent space was excessively good at detecting the signature of an equational theory, see §6.

2. Then, we measured significant differences between the length of an edge associated in the latent space to a reversible proof and to a strict atomic (non reversible) proof. From this follows that provably equivalent theories are tightly clustered together in the latent space, see §7.

3. Finally, we discovered empirically the existence of oriented *implication flows* in the latent space of equational theories, and studied the shape of hard implications, see §8.

This series of converging discoveries indicates an unexpected similitude or correspondence between the purely *model-theoretic* definition of the latent space based on Stone duality, and the purely *proof-theoretic* definition of the implication graph between equational theories. We believe that we only scratched the surface of a statistical variant (and refinement) of the celebrated Gödel completeness theorem for first-order logic, see (Heijenoort, 1967). We include in the Appendix a discussion on Herbrand theorem, which we believe should play a central role in that statistical reconstruction.

These empirical results also convey the hope of enlarging the perspective beyond algebraic reasoning, and defining a *latent space of mathematical concepts* building on the idea of a *universe of types* formulated by Martin-Löf (Martin-Löf, 1975) and recently recast as a *moduli space of types* in Voevodsky's homotopy type theory (Univalent Foundations Program, 2013).

Finally, in a dual and complementary direction, our construction of the latent space of equational theories could provide new tools and insights in the search using reinforcement learning (or other methods) for finite magmas satisfying specific algebraic laws, such as semigroups (Simpson, 2021).

11 Limitations

We introduce the latent space of equational theories and describe its main empiric properties. This is the first paper on the topic, and we thus open a new research area at the interplay of logic and machine learning. For that reason, much remains to be done. The construction of the feature space is simplistic and could be refined by taking random samples of tuples in much larger finite magmas, or on a stochastic and non-deterministic extension of the usual notion of magma. We also used a very elementary linear form of dimensionality reduction based on a PCA method. We could explore other more advanced dimensionality reduction methods such as t-SNE, see (van der Maaten and Hinton, 2008). Although this is mentioned for future work, the current paper does not include any explicit and formal measure of complexity of proofs, such as expansion trees coming from Herbrand theorem. All these limitations can be seen as opening opportunities for future works.

References

Andrea Asperti, Alberto Naibo, and Claudio Sacerdoti Coen. 2025. Thinking machines: Mathematical reasoning in the age of llms. *Preprint*, arXiv:2508.00459.

Matthew Bolan, Jose Brox, Mario Carneiro, Martin Dvorak, Andres Goens, Harald Husum, Zoltan Kocsis, Alex Meiburg, Pietro Monticone, David Renshaw, and 1 others. 2024. The equational theories project: Using lean and github to complete an implication graph in universal algebra. Technical report, Technical report.

Tai-Danae Bradley, Juan Luis Gastaldi, and John Terilla. 2024. The structure of meaning in language: Parallel narratives in linear algebra and category theory. *Notices of the AMS*, 71(2).

Juan Luis Gastaldi and Luc Pellissier. 2021. The calculus of language: explicit representation of emergent linguistic structure through type-theoretical paradigms. *Interdisciplinary Science Reviews*, 46(4):569–590.

Juan Luis Gastaldi and Luc Pellissier. 2023. The Logic of Language: from the Distributional to the Structuralist Hypothesis through Types and Interaction. Working paper or preprint.

Mai Gehrke, Tomáš Jakl, and Luca Reggio. 2022. A duality theoretic view on limits of finite structures: Extended version. *Logical Methods in Computer Science*, Volume 18, Issue 1.

Ayoub El Hanchi, Murat Erdogdu, and Chris Maddison. 2025. A geometric analysis of pca. *arXiv preprint arXiv:2510.20978*.

Jean Van Heijenoort, editor. 1967. *From Frege to Gödel: A Source Book in Mathematical Logic, 1879-1931*. Harvard University Press, Cambridge, MA, USA.

Per Martin-Löf. 1975. An intuitionistic theory of types: Predicative part. In H.E. Rose and J.C. Shepherdson, editors, *Logic Colloquium '73*, volume 80 of *Studies in Logic and the Foundations of Mathematics*, pages 73–118. Elsevier.

Dale A. Miller. 1987. A compact representation of proofs. *Studia Logica: An International Journal for Symbolic Logic*, 46(4):347–370.

Jaroslav Nešetřil and Patrice Ossona de Mendez. 2012. A model theory approach to structural limits. *Commentationes Mathematicae Universitatis Carolinae*, 53(4):581–603.

Jaroslav Nešetřil and Patrice Ossona de Mendez. 2020. A unified approach to structural limits and limits of graphs with bounded tree-depth. *Memoirs of the American Mathematical Society*, 263(1272):0–0.

Jonathon Shlens. 2014. A tutorial on principal component analysis. *arXiv preprint arXiv:1404.1100*.

Carlos Simpson. 2021. Learning proofs for the classification of nilpotent semigroups. *CoRR*, abs/2106.03015.

The Univalent Foundations Program. 2013. *Homotopy Type Theory: Univalent Foundations of Mathematics*. `https://homotopytypetheory.org/book`, Institute for Advanced Study.

Laurens van der Maaten and Geoffrey Hinton. 2008. Visualizing data using t-sne. *Journal of Machine Learning Research*, 9(86):2579–2605.

Yufa Zhou, Yixiao Wang, Xunjian Yin, Shuyan Zhou, and Anru R Zhang. 2025. The geometry of reasoning: Flowing logics in representation space. *arXiv preprint arXiv:2510.09782*.

A Linear regression graphs for the first and second principal components X and Y

We provide in Fig. 8 and Fig. 9 the linear regression graphs mentioned in §6.4 and in §6.5.

B Cliques of provably equivalent theories

The repartition of reversible cliques follows:

	1	2	3	4	5	6	7	8	9	12	14	18	27	30	31	37	40	71	76	112	419	1496
1	2717	312	102	36	80	48	0	64	108	0	0	0	0	0	0	0	0	0	0	0	0	0
2	1174	164	156	144	0	48	0	0	0	0	0	0	0	0	248	0	0	0	0	0	0	0
3	813	378	225	48	30	36	0	0	0	0	0	0	0	0	0	0	0	0	0	0	0	0
4	328	64	24	32	0	48	0	0	0	0	0	0	0	0	0	0	0	0	0	0	0	0
5	410	200	120	0	0	0	0	0	0	0	0	0	0	0	0	0	0	0	0	0	0	0
6	606	228	234	96	0	216	0	96	0	72	0	0	0	180	0	0	0	0	0	0	0	0
7	70	252	84	0	0	0	0	0	0	0	0	0	0	0	0	0	0	0	0	0	0	0
8	512	80	240	0	0	0	0	64	0	0	0	0	0	0	0	0	0	0	0	0	0	0
9	486	216	54	0	0	0	0	0	0	0	0	0	0	0	0	0	0	0	0	0	0	0
12	252	72	0	0	0	0	0	0	0	0	0	0	0	0	0	0	0	0	0	0	0	0
14	14	56	0	0	350	0	196	0	0	0	0	0	0	0	0	0	0	0	0	0	0	0
18	72	0	108	144	0	0	0	0	0	0	0	0	0	0	0	0	0	0	0	0	0	0
27	216	0	324	0	0	0	0	0	0	0	0	0	0	0	0	0	1440	0	0	0	0	0
30	510	300	0	0	0	0	0	480	0	0	0	0	0	0	0	0	2160	0	0	0	0	0
31	62	372	372	0	0	0	0	992	0	0	0	0	0	0	0	0	0	0	0	0	0	0
37	370	296	0	0	0	0	0	0	0	0	0	1332	0	0	0	0	0	0	0	0	0	0
40	240	320	0	0	0	0	0	640	0	0	0	0	0	0	0	0	0	0	0	0	0	0
71	1704	0	426	568	0	0	0	0	0	0	0	0	0	0	0	5254	0	0	10792	15904	0	0
76	760	608	912	608	0	0	0	0	0	0	0	0	0	0	0	0	6080	0	0	0	0	0
112	2016	1792	672	0	0	1344	1568	0	2016	0	0	4032	6048	0	0	0	0	0	0	0	0	0
419	4609	1676	1257	0	0	2514	0	0	0	0	5866	0	0	0	0	31006	0	0	0	0	0	626824
1496	59840	0	4488	5984	0	8976	0	0	0	0	0	0	0	0	0	0	0	212432	0	0	626824	0

Table 1: Depicts the number of strict edges from each reversible to another.

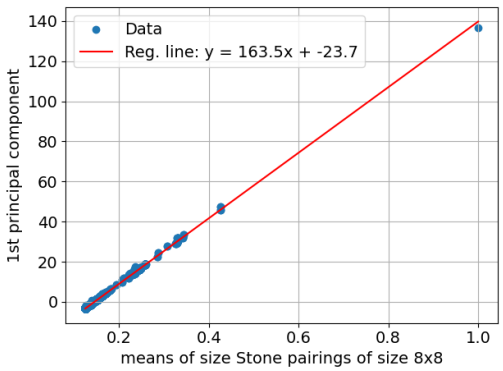

Figure 8: Linear regression graph of the expectation (or mean) of the Stone pairing for each equational theory with relation to the first principal component X.

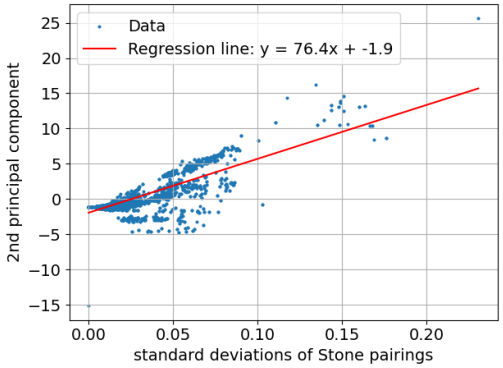

Figure 9: Regression graph of the standard value of the Stone pairings for each equation vrs. the second principal component Y.

cardinal of the clique	number of cliques of this cardinal	number of vertices
1496	1	1496
419	1	419
112	2	224
76	2	152
71	2	142
40	2	80
37	2	74
31	2	62
30	1	30
27	2	54
18	2	36
14	1	14
12	1	12
9	4	36
8	7	56
7	4	28
6	11	66
5	11	55
4	14	56
3	61	183
2	137	274
1	1145	1145

size of clique	selected equation in the clique	
1496	Eqn[1]	$x = y$
419	Eqn[45]	$x \diamond y = z \diamond w$
112	Eqn[18]	$x = y \diamond (z \diamond x)$
112	Eqn[26]	$x = (x \diamond y) \diamond z$
76	Eqn[93]	$x = y \diamond (z \diamond (w \diamond x))$
76	Eqn[268]	$x = ((x \diamond y) \diamond z) \diamond w$
71	Eqn[3]	$x = x \diamond y$
71	Eqn[4]	$x = y \diamond x$
40	Eqn[41]	$x \diamond y = x \diamond z$
40	Eqn[44]	$x \diamond y = z \diamond y$
37	Eqn[354]	$x \diamond y = z \diamond (w \diamond y)$
37	Eqn[382]	$x \diamond y = (x \diamond z) \diamond w$
31	Eqn[4378]	$x \diamond (y \diamond z) = w \diamond (u \diamond v)$
31	Eqn[4693]	$(x \diamond y) \diamond z = (w \diamond u) \diamond v$
30	Eqn[710]	$x = y \diamond (y \diamond ((x \diamond z) \diamond z))$
	Eqn[2943]	$x = ((y \diamond (y \diamond x)) \diamond z) \diamond z$
27	Eqn[607]	$x = y \diamond (z \diamond (w \diamond (u \diamond x)))$
27	Eqn[3100]	$x = (((x \diamond y) \diamond z) \diamond w) \diamond u$
18	Eqn[3450]	$x \diamond y = z \diamond (w \diamond (u \diamond y))$
18	Eqn[4152]	$x \diamond y = ((x \diamond z) \diamond w) \diamond u$
14	Eqn[4581]	$x \diamond (y \diamond z) = (w \diamond u) \diamond v$
12	Eqn[1354]	$x = y \diamond (((z \diamond x) \diamond y) \diamond z)$
	Eqn[2369]	$x = (y \diamond (z \diamond (x \diamond y))) \diamond z$
9	Eqn[8]	$x = x \diamond (x \diamond y)$
9	Eqn[27]	$x = (y \diamond x) \diamond x$
9	Eqn[1815]	$x = (y \diamond z) \diamond ((w \diamond z) \diamond x))$
9	Eqn[1873]	$x = (x \diamond (y \diamond z)) \diamond (y \diamond w)$
8	Eqn[13]	$x = y \diamond (x \diamond y)$
	Eqn[28]	$x = (y \diamond x) \diamond y$
8	Eqn[745]	$x = y \diamond (z \diamond (x \diamond y) \diamond z)$
	Eqn[2978]	$x = ((y \diamond (z \diamond x)) \diamond y) \diamond z$
8	Eqn[3369]	$x \diamond y = y \diamond (z \diamond (z \diamond x))$
	Eqn[4181]	$x \diamond y = ((y \diamond z) \diamond z) \diamond x$
8	Eqn[4360]	$x \diamond (y \diamond z) = x \diamond (w \diamond u)$
8	Eqn[4692]	$(x \diamond y) \diamond z = (w \diamond u) \diamond z$
8	Eqn[4377]	$x \diamond (y \diamond z) = w \diamond (u \diamond z)$
8	Eqn[4675]	$(x \diamond y) \diamond z = (x \diamond w) \diamond u$
7	Eqn[160]	$x = (x \diamond y) \diamond (y \diamond z)$
7	Eqn[193]	$x = (y \diamond z) \diamond (z \diamond x)$
7	Eqn[4467]	$x \diamond (y \diamond x) = (z \diamond w) \diamond u$
7	Eqn[4579]	$x \diamond (y \diamond z) = (w \diamond u) \diamond w$

Figure 10: List of all equivalence classes of equational theories modulo $\sim$, of size between 7 and 1496, together with one or two distinctive elements of each clique.

C Herbrand theorem and parallelism of implication flows

Suppose given a pair of magma equations

$$\varphi(\mathbf{u}) = \varphi(u_1, \ldots, u_k)$$

where φ has free variables $\mathbf{u} = (u_1, \ldots, u_k)$ and

$$\psi(\mathbf{x}) = \psi(x_1, \ldots, x_\ell).$$

where ψ has free variables $\mathbf{x} = (x_1, \ldots, x_\ell)$.

A Herbrand proof

$$(\theta_1, \ldots, \theta_n) \quad : \quad \forall \mathbf{u}.\varphi(\mathbf{u}) \ \vdash \ \forall \mathbf{x}.\psi(\mathbf{x})$$

is defined as a finite sequence $(\theta_1, \ldots, \theta_n)$ where each θ_i is a substitution of the free variables

$$\mathbf{u} = (u_1, \ldots, u_k)$$

of the equation φ with magma expressions parametrized by the free variables

$$\mathbf{x} = (x_1, \ldots, x_\ell)$$

of the equation ψ, such that one can establish

$$\forall \mathbf{x}. \ \Big(\ \varphi[\theta_1] \wedge \cdots \wedge \varphi[\theta_n] \ \Big) \ \Rightarrow \ \phi(\mathbf{x}).$$

Consider for instance Eqn[13]

$$\forall \mathbf{u}.\, \varphi(\mathbf{u}) \quad \equiv \quad \forall u.v. \ u = v \diamond (u \diamond v)$$

and Eqn[1557]

$$\forall \mathbf{x}.\, \psi(\mathbf{x}) \ \equiv \ \forall x.y.z. \ x = (y \diamond z) \diamond (x \diamond (y \diamond z))$$

with free variables $\mathbf{u} = (u, v)$ and $\mathbf{x} = (x, y, z)$, respectively. In one direction, the fact that Eqn[13] implies Eqn[1557] is obvious by substituting the two variables u and v with the expressions

$$\theta : u \mapsto x \quad \text{and} \quad \theta : v \mapsto x \diamond y.$$

From this, one concludes that the substitution θ establishes the implication:

$$\theta \quad : \quad \mathsf{Eqn}[13] \ \vdash \ \mathsf{Eqn}[1557]$$

Conversely, somewhat surprisingly, the Equational Theories project indicates that Eqn[1557] implies Eqn[13]. This nontrivial fact can be established by applying the pair of substitutions

$$\theta_1 \ : \ x \mapsto u, \quad y \mapsto u \diamond v, \quad z \mapsto v \diamond (u \diamond u)$$

$$\theta_2 \ : \ x \mapsto v, \quad y \mapsto u, \quad z \mapsto u.$$

to the equation

$$\psi(x, y, z) \quad \equiv \quad x \ = \ (y \diamond z) \diamond (x \diamond (y \diamond z))$$

in order to obtain the equation $\psi[\theta_1]$ after substitution by θ_1:

$u = ((u \diamond u) \diamond (v \diamond (u \diamond u))) \diamond (u \diamond ((u \diamond u) \diamond (v \diamond (u \diamond u))))$

and the equation $\psi[\theta_2]$ after substitution by θ_2:

$$v = (u \diamond u) \diamond (v \diamond (u \diamond u))$$

An easy equational reasoning establishes that the pair of the two equations implies $\mathsf{Eqn}[13]$:

$$\varphi(u, v) \quad \equiv \quad u = v \diamond (u \diamond v) \qquad (2)$$

From this, one concludes that

$$(\theta_1, \theta_2) \quad : \quad \mathsf{Eqn}[1557] \ \vdash \ \mathsf{Eqn}[13]$$

Note that the two substitutions θ_3 and θ_4 defined below would establish (2) in just the same way:

$$\theta_3 \ : \ x \mapsto u, \quad y \mapsto u \diamond v, \quad z \mapsto v \diamond (u \diamond u)$$

$$\theta_4 \ : \ x \mapsto v, \quad y \mapsto u, \quad z \mapsto v.$$

From this follows that

$$(\theta_3, \theta_4) \quad : \quad \mathsf{Eqn}[1557] \ \vdash \ \mathsf{Eqn}[13]$$

This defines a category with equations as objects and Herbrand proofs as morphisms. The fact that $(\theta_1, \theta_2) \neq (\theta_3, \theta_4)$ means that this is a category and not just a preorder.

There are special commutative triangles:

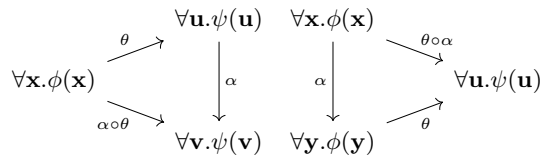

where the sides are linear substitutions. These deserve to be filled, in order to define a higher-dimensional manifold (defined as a simplicial set) of equations and reasonings, constructed as a variation of the nerve of a category. We leave that for future work.